Strong enhancement of spin ordering by A-site magnetic ions in the ferrimagnet CaCu$_3$Fe$_2$Os$_2$O$_{12}$

Hongshan Deng,[1,2] Min Liu,[1] Jianhong Dai,[1] Zhiwei Hu,[3] Changyang Kuo,[3] Yunyu Yin,[1] Junye Yang,[1] Xiao Wang,[1]
Qing Zhao,[1] Yuanji Xu,[1] Zhaoming Fu,[1] Jianwang Cai,[1] Haizhong Guo,[1] Kuijuan Jin,[1,4] Tunwen Pi,[5] Yunliang Soo,[5,6]
Guanghui Zhou,[2] Jinguang Cheng,[1] Kai Chen,[7] Philippe Ohresser,[7] Yi-feng Yang,[1,4,*] Changqing Jin,[1,4]
Liu-Hao Tjeng,[3] and Youwen Long[1,4,†]

[1]*Beijing National Laboratory for Condensed Matter Physics, Institute of Physics, Chinese Academy of Sciences, Beijing 100190, China*
[2]*Department of Physics and Synergetic Innovation Center for Quantum Effects and Applications of Hunan,*
Hunan Normal University, Changsha 410081, China
[3]*Max-Planck Institute for Chemical Physics of Solids, Nöthnitzer Straße 40, 01187 Dresden, Germany*
[4]*Collaborative Innovation Center of Quantum Matter, Beijing 100190, China*
[5]*National Synchrotron Radiation Research Center, Hsinchu 30076, Taiwan*
[6]*Department of Physics, National Tsing Hua University, Hsinchu 30013, Taiwan*
[7]*Synchrotron SOLEIL, L'Orme des Merisiers, Saint-Aubin-BP 48, 91192 Gif-sur-Yvette Cedex, France*

ABO$_3$ perovskite is a kind of very important functional material with versatile physical properties. Although B-site chemical substitution with various magnetic ions has been widely investigated, the A-site doping with magnetic transition metal is little known. Here we report $AA'_3B_2B'_2$O$_{12}$-type A- and B-site ordered ferrimagnet CaCu$_3$Fe$_2$Os$_2$O$_{12}$ with magnetic transition metals occupying three different atomic sites (A', B, and B' sites). This compound is synthesized by a special high-pressure annealing process. It possesses a much higher Curie temperature T_C of 580 K compared with that of the B-site-only ordered Ca$_2$FeOsO$_6$ ($T_C = 320$ K) without magnetic ion at the A site. First-principles numerical calculations reveal that this enhancement primarily originates from the additional spin interaction between the A'-site Cu^{2+} and the B'-site Os^{5+}, generating a strong Cu$^{2+}(\uparrow)$Fe$^{3+}(\uparrow)$Os$^{5+}(\downarrow)$ ferrimagnetic spin coupling. This work opens up an alternative way for enhancing the spin ordering temperature by introducing A-site magnetic ions.

I. INTRODUCTION

In the past decades ABO$_3$ perovskite oxides have received much attention due to the wide variety of physical properties and fascinating functionalities such as piezoelectricity, ferroelectricity, superconductivity, colossal magnetoresistance, and multiferroicity, etc. [1–5]. For the practical utilization of these performances, a high phase transition temperature near or even above room temperature (RT) is generally required. Since the crystal structure and the A-B charge combination in a perovskite is highly flexible, B-site chemical doping has been studied widely to design ordered perovskite materials with high charge and/or spin ordering temperatures. One interesting example is the half-metallic ferrimagnetic (FiM) compound Sr$_2$FeMoO$_6$, the so-called B-site ordered double perovskite (DP) with T_C about 420 K [6]. This relatively high T_C has stimulated considerable efforts on preparing 3d-4d and 3d-5d hybrid magnetic materials with high ordering temperatures. Very recently the B-site ordered DPs A_2FeOsO$_6$ (A = Ca, Sr) have received particular attention due to the diverse competing interactions in spin, orbital, and lattice degrees of freedom [7–12]. The tetragonal Sr$_2$FeOsO$_6$ exhibits two successive antiferromagnetic (AFM) transitions on cooling to about 140 and 67 K, respectively, whereas a high-temperature FiM ordering ($T_C \approx 320$ K) is found to occur in Ca$_2$FeOsO$_6$ driven by further lattice distortion [7–9].

In ABO$_3$ perovskite, while the B site can be occupied by various magnetic transition metals, the A site usually accommodates nonmagnetic alkali metal, alkaline earth, and/or lanthanide cations. Therefore, A-site chemical substitution with magnetic ions is at present less studied. However, for a B-site ordered DP A_2BB'O$_6$, if three-quarters of the A sites are substituted by a transition-metal A', both an A- and B-site ordered quadruple perovskite (QP) with chemical formula of $AA'_3B_2B'_2$O$_{12}$ can form [13–19]. A unique feature for this specially ordered perovskite is that three different atomic sites (A', B, and B' sites) can all accommodate magnetic transition metals [see Fig. 1(a)]. As a consequence, multiple magnetic and electrical interactions can occur among A', B, and/or B' sites, giving rise to a series of intriguing physical phenomena such as intersite charge transfer, charge disproportionation, spin-induced ferroelectricity, and FiM half-metallicity [20–24]. Besides, it is also highly expected that the strong coupling among these magnetic sublattices has important impacts on further enhancing the spin or charge ordering temperature.

In the ordered $AA'_3B_2B'_2$O$_{12}$ perovskite, the A-site substitution with smaller-size transition metal significantly decreases the average ionic radius for this atomic site. The B/B'O$_6$ octahedra thus become heavily tilting (typically, $\angle B/B'$-O-$B/B' \approx 140°$) and the A'-site transition metal forms square-planar coordinated A'O$_4$ units. As a result, high pressure is often needed to prepare the A- and B-site ordered perovskite. To date, although a large number of ABO$_3$ perovskites and B-site only ordered DPs have already been obtained, the family members of both A-site and B-site ordered QPs are very limited. In this paper, we report an A- and B-site
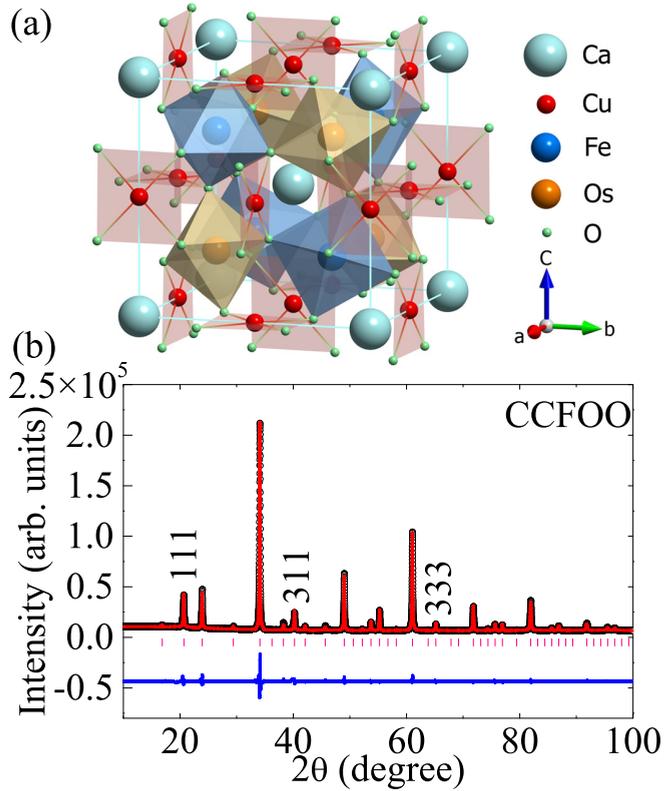
*yifeng@iphy.ac.cn
†ywlong@iphy.ac.cn

FIG. 1. (a) Schematic of crystal structure of the A- and B-site ordered $AA'_3B_2B'_2O_{12}$-type quadruple perovskite $CaCu_3Fe_2Os_2O_{12}$. The corner-sharing Fe/OsO_6 octahedra and spatially isolated CuO_4 squares are shown. (b) XRD pattern and structure refinement results obtained at room temperature. The observed (circles), calculated (red line), and difference (bottom line) are shown. The ticks indicate the allowed Bragg reflections with space group Pn-3.

ordered QP oxide, $CaCu_3Fe_2Os_2O_{12}$ (CCFOO). The advantage of both A- and B-site ordered CCFOO as compared with the B-site-only ordered Ca_2FeOsO_6 is clearly seen by the sharp enhancement of the FiM ordering temperature from 320 K in the latter to 580 K in the former due to the introduction of extra spin interactions related to the A'-site Cu^{2+} ions. The strong $Cu^{2+}(\uparrow)Fe^{3+}(\uparrow)Os^{5+}(\downarrow)$ FiM spin coupling as well as the detailed electronic properties are also studied by first-principles numerical calculations. The present study illuminates that A-site substitution with magnetic ions can be applied as an effective method to search perovskite functional materials with enhanced ordering temperature well above RT.

II. EXPERIMENTAL AND CALCULATION DETAILS

The polycrystalline sample of $CaCu_3Fe_2Os_2O_{12}$ was prepared by a high-pressure annealing method. High-purity (>99.9%) CaO, CuO, Fe_2O_3, and Os powders with a mole ratio of 1:3:1:2 were used as starting materials, and appropriate $KClO_4$ was adopted as an oxidizing agent. These reactants were thoroughly mixed in an agate mortar. The mixed powders were then pressed into a Pt capsule 3 mm in diameter and 4 mm in length for high-pressure and high-temperature treatment by using a cubic-anvil-type high-pressure apparatus. At the

optimal pressure (8–10 GPa), the mixed reactants were heated at 1573 K for 30 min, and then the temperature was slowly decreased to 1073 K within 6 h. When this annealing process was finished, the heating power was shut down quickly, and then the pressure was gradually released. The residual KCl in the final product was washed out by de-ionized water.

The sample quality and crystal structure were characterized by powder x-ray diffraction (XRD) using a Huber diffractometer (Cu $K\alpha_1$ radiation, 40 kV, 300 mA). Diffraction data were collected in the angle (2θ) range from 10° to 100° with steps of 0.01°. Crystallographic parameters were analyzed by Rietveld full-profile refinement using the GSAS program [25]. The valence states of Cu, Fe, and Os transition metals were identified by x-ray absorption spectra (XAS) performed at the National Synchrotron Radiation Research Center in Taiwan. The soft XAS at the Cu- and Fe-$L_{2,3}$ edges were measured with total electron yield at the beamline of BL08B. The hard XAS at the Os-$L_{2,3}$ edges were measured with transmission geometry at the BL07A beamline. X-ray magnetic circular dichroism (XMCD) measurements at the Cu- and Fe-$L_{2,3}$ edges were performed at the Deimos beamline of SOLEIL in Paris. The spectra were taken with circularly polarized x rays at 132 K and 2 T magnetic field considering that the sample was charging at low temperature and high magnetic field due to strong insulator and magnetoresistance effects.

Magnetic susceptibility and magnetization below 400 K were measured using a Quantum Design superconducting quantum interference device magnetometer. The data of high-temperature susceptibility in the 400–650 K range were collected using a MicroSense vibrating sample magnetometer. The zero-field-cooling (ZFC) and field-cooling (FC) modes were adopted for magnetic susceptibility measurements with a 0.1-T magnetic field. The resistivity was measured by adopting a four-probe method on a Quantum Design physical property measurement system. The photocurrent measurement was performed using a laser (PL2210A, PG403-SH, and PG703-DFG, EKSPLA), varying the wavelengths from 1.80 to 0.55 μm at room temperature. The photovoltaic signals were recorded by a Keithley 2400 electrometer.

First-principles numerical calculations were performed using the full-potential linearized augmented plane-wave method implemented in WIEN2K [26]. The lattice parameters and atom positions obtained in experiment were used for the numerical calculations. The structure optimization gives the lattice parameter $a = 7.523$ Å and the O atomic position to be 0.254, 0.426, and 0.555. The muffin-tin radii were 2.00 a.u. for Ca; 1.60 a.u. for O; and 1.90 for Cu, Fe, and Os. The maximum modulus for the reciprocal vectors K_{max} was chosen such that $R_{MT}K_{max} = 7.0$. A different value of $R_{MT}K_{max} = 8.0$ was also tested and no significant changes were observed except slight variations in the energy convergence. We took the generalized-gradient approximation Perdew-Burke-Ernzerhof (GGA-PBE) exchange-correlation energy and used 1000 k-point meshes for the whole Brillouin zone, with an effective $U_{eff} = 5$ eV for Cu, 4 eV for Fe, and 2 eV for Os in the GGA + U calculations. The nearest-neighbor effective exchange couplings between magnetic ions were calculated using the energy difference of four different magnetic structures [FiM1: $Cu^{2+}(\uparrow)Fe^{3+}(\uparrow)Os^{5+}(\downarrow)$; FiM2: $Cu^{2+}(\uparrow)Fe^{3+}(\downarrow)Os^{5+}(\downarrow)$; FiM3: $Cu^{2+}(\downarrow)Fe^{3+}(\uparrow)Os^{5+}(\downarrow)$;

FM: $Cu^{2+}(\uparrow)Fe^{3+}(\uparrow)Os^{5+}(\uparrow)$]:

$$E(\text{FiM1}) = E_0 + 12J_{\text{Cu-Fe}}S_{\text{Cu}}S_{\text{Fe}}$$
$$- 12J_{\text{Fe-Os}}S_{\text{Fe}}S_{\text{Os}} - 12J_{\text{Cu-Os}}S_{\text{Cu}}S_{\text{Os}},$$

$$E(\text{FiM2}) = E_0 - 12J_{\text{Cu-Fe}}S_{\text{Cu}}S_{\text{Fe}}$$
$$+ 12J_{\text{Fe-Os}}S_{\text{Fe}}S_{\text{Os}} - 12J_{\text{Cu-Os}}S_{\text{Cu}}S_{\text{Os}},$$

$$E(\text{FiM3}) = E_0 - 12J_{\text{Cu-Fe}}S_{\text{Cu}}S_{\text{Fe}}$$
$$- 12J_{\text{Fe-Os}}S_{\text{Fe}}S_{\text{Os}} + 12J_{\text{Cu-Os}}S_{\text{Cu}}S_{\text{Os}},$$

$$E(\text{FM}) = E_0 + 12J_{\text{Cu-Fe}}S_{\text{Cu}}S_{\text{Fe}}$$
$$+ 12J_{\text{Fe-Os}}S_{\text{Fe}}S_{\text{Os}} + 12J_{\text{Cu-Os}}S_{\text{Cu}}S_{\text{Os}}.$$

III. RESULTS AND DISCUSSION

Figure 1(b) shows the XRD pattern of CCFOO measured at room temperature. The presence of the sharp diffraction peaks with $h + k + l = $ odd such as (111) and (311) peaks provides convincing evidence for the rocksalt-type ordered arrangement of Fe and Os cations [15]. The Rietveld analysis illustrates that the high-pressure product CCFOO crystallizes to an $AA'_3B_2B'_2O_{12}$-type A-site and B-site ordered quadruple perovskite structure with space group Pn-3 [see Fig. 1(a)]. In this structural symmetry, the A-site Ca and A'-site Cu atoms occupy the fixed atomic sites $2a$ (0.25, 0.25, 0.25) and $6d$ (0.25, 0.75, 0.75), and the B-site Fe and B'-site Os atoms are in an orderly distribution at the $4b$ (0, 0, 0) and $4c$ (0.5, 0.5, 0.5) sites, respectively. Detailed structure refinements for the occupancy factors of cations show a nearly ideal 1:3 ordering between the A-site Ca and the A'-site Cu atoms (i.e., there is neither Ca-Cu antisite occupancy nor other elements occupying these two sites), while a small amount of Fe-Os antisite occupancy is found to occur by about 11%. The refined structural parameters are listed in Table I. Based on the related bond lengths, the bond valence sum (BVS) calculations respectively give the valence states of Cu, Fe, and Os to be 2.11, 2.87, and 5.23, indicating a $CaCu^{2+}_3Fe^{3+}_2Os^{5+}_2O_{12}$ charge combination, in agreement with the XAS measurements shown below.

The x-ray absorption spectrum at the $3d$ transition-metal $L_{2,3}$ edges is highly sensitive to the valence state as well as the local environment of the transition metal. Figure 2(a) shows the Cu-$L_{2,3}$ XAS of CCFOO together with Cu_2O, CuO, and $NaCuO_2$ as pure Cu^{1+}, Cu^{2+}, and Cu^{3+} references, respectively [27,28]. Obviously, the spectrum of $NaCuO_2$ is shifted by 1.8 eV to higher energy relative to that of CuO. The weak, but highest, energy of the Cu_2O spectrum is assigned to the s-related states since the $3d$ states are fully occupied for the $3d^{10}$ electronic configuration of Cu^{1+}. One can see a sharp and symmetric peak at the Cu-$L_{2,3}$ edges of CCFOO at an similar energy similar to that of CuO, but no Cu^{1+}- and Cu^{3+}-related spectral feature demonstrating the same Cu^{2+} valence state [27–30]. Note that the CCFOO spectrum is shifted by about 0.45 eV to lower energy with respect to the CuO spectrum, reflecting different Cu local environments. The unoccupied $d(x^2-y^2)$ orbital is expected to have a lower energy in CCFOO than that in CuO due to a longer Cu-O distance and a square-planar coordination in the former.

Figure 2(b) shows the Fe-$L_{2,3}$ XAS of CCFOO together with $Fe_{0.04}Mg_{0.96}O$ [31] and Fe_2O_3 as high-spin Fe^{2+} and Fe^{3+}

TABLE I. Refined structure parameters of CCFOO and the BVS values for Cu, Fe, and Os at room temperature. Space group: Pn-3; atomic sites: Ca $2a$ (0.25, 0.25, 0.25); Cu $6d$ (0.25, 0.75, 0.75); Fe $4b$ (0, 0, 0); Os $4c$ (0.5, 0.5, 0.5); O $24g$ (x, y, z). The BVS values (V_i) were calculated using the formula $V_i = \sum_j S_{ij}$, and $S_{ij} = \exp[(r_0 - r_{ij})/0.37]$. The value of $r_0 = 1.679$ for Cu, 1.759 for Fe, and 1.868 for Os. For the B-site Fe and B'-site Os, six coordinated oxygen atoms were used. For the A'-site Cu, twelve coordinated oxygen atoms were used. G: site occupancy.

Parameter	CCFOO
a (Å)	7.43264(3)
O_x	0.2580(3)
O_y	0.4304(5)
O_z	0.5574(4)
G ($2a$ for Ca)	1.009(8)
G ($6d$ for Cu)	1.035(3)
G ($4b$ for Fe1)	0.882(1)
G ($4b$ for Os1)	0.118(1)
G ($4c$ for Os2)	0.882(1)
G ($4c$ for Fe2)	0.118(1)
U_{iso} (Ca) ($100 \times$ Å^2)	0.01
U_{iso} (Cu) ($100 \times$ Å^2)	0.53(4)
U_{iso} (Fe1) ($100 \times$ Å^2)	0.01
U_{iso} (Os2) ($100 \times$ Å^2)	0.72(2)
U_{iso} (O) ($100 \times$ Å^2)	0.01
Cu-O ($\times 4$) (Å)	1.963(2)
Fe1-O ($\times 6$) (Å)	2.032(2)
Os2-O ($\times 6$) (Å)	1.919(2)
$\angle$Fe1-O-Os2 (deg)	140.3(1)
$\angle$Cu-O-Fe1 (deg)	107.4(1)
$\angle$Cu-O-Os2 (deg)	112.0(1)
BVS (Cu)	2.11
BVS (Fe)	2.87
BVS (Os)	5.23
R_{wp} (%)	4.13
R_{p} (%)	2.93

references with FeO_6 octahedral coordination, respectively. The same energy position and very similar line shape of both CCFOO and Fe_2O_3, but 1.9 eV lower than that of Fe^{2+} reference $Fe_{0.04}Mg_{0.96}O$, demonstrate a high-spin Fe^{3+} state in CCFOO. We now turn to the Os-$L_{2,3}$ XAS analysis. In Fig. 2(c) one can find that the white line in the Os-L_3 edge of CCFOO lies at the same energy position as that of Sr_2FeOsO_6 known with Fe^{3+}/Os^{5+} charge states and 1.2 eV above Os^{4+} reference La_2MgOsO_6 conforming the formation of Os^{5+} in the present CCFOO [32]. Therefore, XAS measurements give unambiguous evidence for the presence of Cu^{2+}/Fe^{3+}/Os^{5+} valence states in the A- and B-site ordered CCFOO.

The magnetism of CCFOO was characterized by field-dependent magnetization measurements as shown in Fig. 3(a). The presence of canonical magnetic hysteresis loops at several selected temperatures reveals the ferromagnetic (FM) or FiM behavior. The saturated moment obtained at 2 K is about 5.0 μ_B/f.u. Even at 400 K, a considerable saturated moment can be observed (2.5 μ_B/f.u.), indicating strong FM/FiM interactions. In addition, we find a moderate coercive force
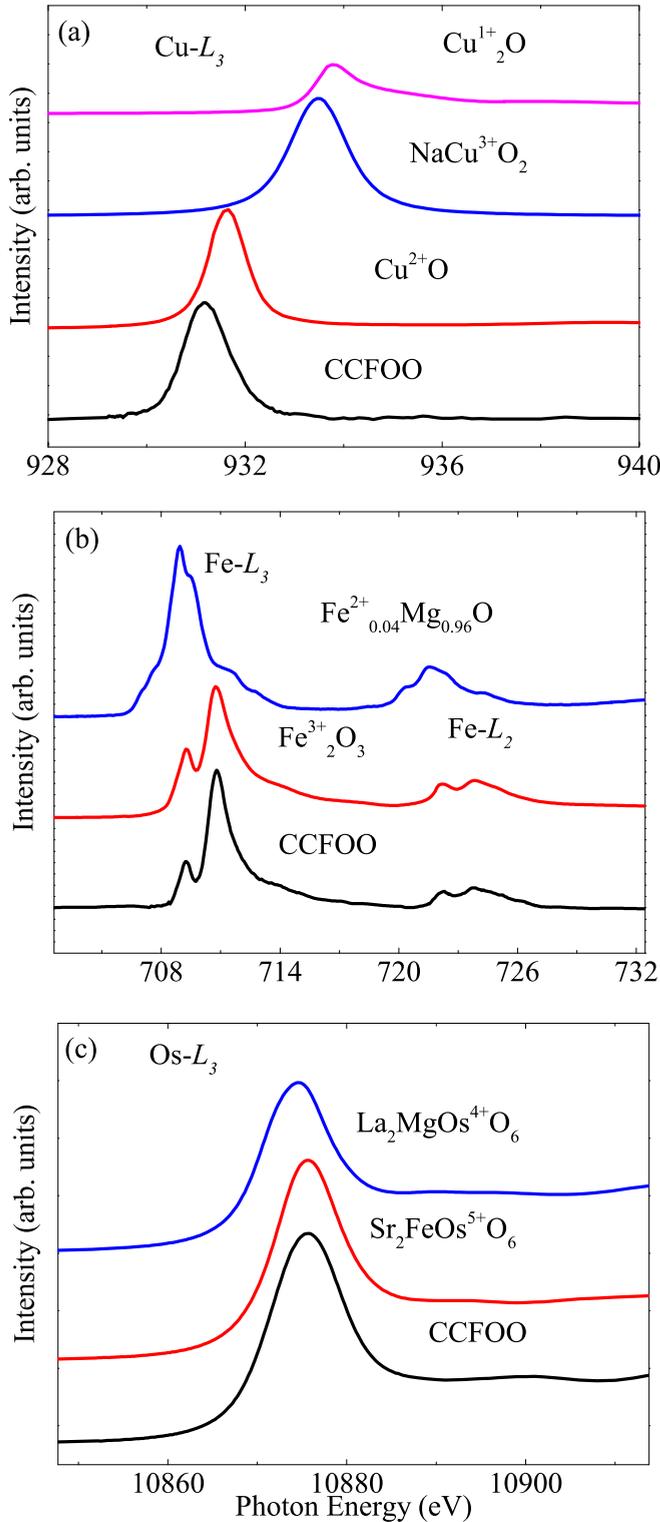
FIG. 2. (a) XAS of Cu-$L_{2,3}$ edges, (b) Fe-$L_{2,3}$ edges, and (c) Os-L_3 edges. The XAS of related references are also shown for comparison.
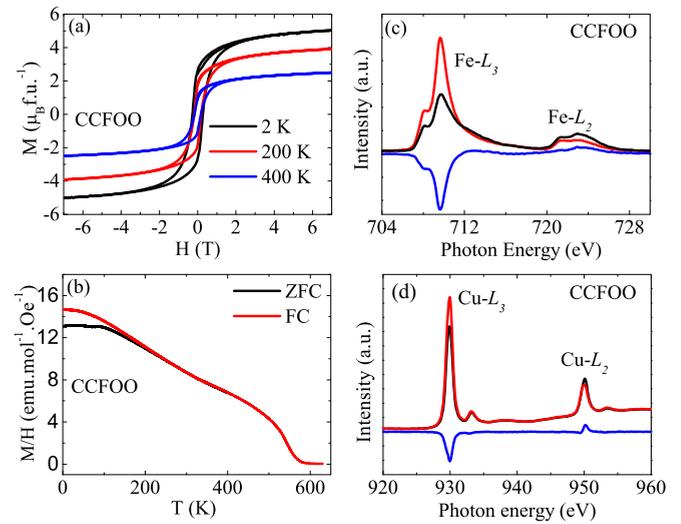

FIG. 3. (a) Field-dependent magnetization measured at different temperatures. (b) Temperature-dependent magnetic susceptibility measured at 0.1 T with ZFC and FC modes. (c,d) XMCD for Fe- and Cu-$L_{2,3}$ edges. The photon spin is aligned parallel (μ^+ black line) and antiparallel (μ^- red line) to the applied magnetic field, respectively. The difference spectra are shown in blue.

increase at the onset of about 580 K, revealing strong FM or FiM coupling as demonstrated by the magnetization results mentioned above. The present CCFOO possesses a high T_C in the A-site ordered and B-site ordered or disordered QPs; compare [13–22,33–38].

In CCFOO, all the transition-metal ions Cu^{2+} ($S_{Cu} = 1/2$), Fe^{3+} ($S_{Fe} = 5/2$), and Os^{5+} ($S_{Os} = 3/2$) can possibly take part in the spin interactions. Both the collinear $Cu^{2+}(\uparrow)Fe^{3+}(\uparrow)Os^{5+}(\uparrow)$ FM state and the FiM $Cu^{2+}(\uparrow)Fe^{3+}(\downarrow)Os^{5+}(\downarrow)$ state produce unreasonably large saturated moments (19.0 and 13.0 μ_B/f.u., respectively) with regard to the experimental observation in the assumption of local-electron model without considering the spin-orbital coupling (SOC) of Os^{5+}. Actually, the SOC effect of Os^{5+} is not significant due to the d^3-electron configuration as confirmed by theoretical calculations [7,9,11,12,32]. In addition, the FiM coupling of $Cu^{2+}(\downarrow)Fe^{3+}(\uparrow)Os^{5+}(\downarrow)$ gives a too small spin moment (1.0 μ_B/f.u.). In comparison, only the $Cu^{2+}(\uparrow)Fe^{3+}(\uparrow)Os^{5+}(\downarrow)$ FiM state yields a spin moment (7.0 μ_B/f.u.) that is comparable with the experimental value obtained at 2 K (5.0 μ_B/f.u.). The small amount of Fe-Os antioccupancy as well as the strong hybridization between the Os-$5d$ and O-$2p$ orbitals (shown later) should be responsible for the reduced spin moment observed in experiment. Furthermore, the $Cu^{2+}(\uparrow)Fe^{3+}(\uparrow)$ FM alignment can be confirmed by XMCD measurement at the Cu- and Fe-$L_{2,3}$ edges. As seen in Figs. 3(c) and 3(d), the same sign of XMCD spectra at the Fe- and Cu-$L_{2,3}$ edges reveals the FM coupling between the A'-site Cu^{2+} and the B-site Fe^{3+} ions, in coherence with the proposed $Cu^{2+}(\uparrow)Fe^{3+}(\uparrow)Os^{5+}(\downarrow)$ ferrimagnetic spin alignment.

The resistivity of CCFOO was measured on a polycrystalline pellet pressed under 6 GPa. As shown in the inset of Fig. 4, the magnitude of resistivity gradually increases with decreasing temperature and reaches $10^4 \Omega$ cm at low temperatures, suggesting the semiconducting or insulating
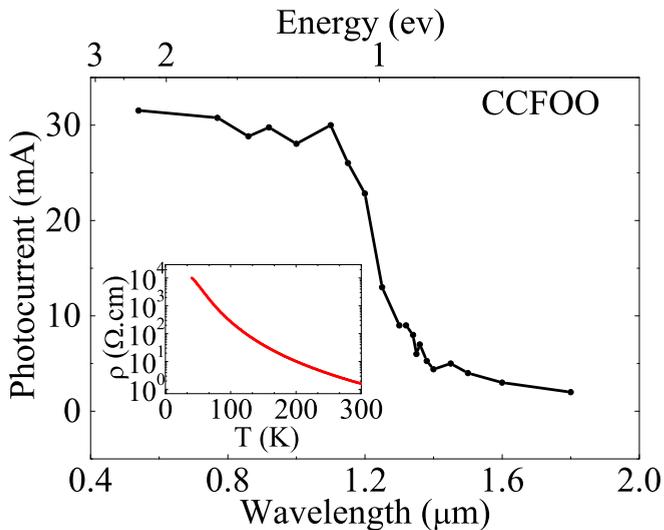
($\sim$0.27 T at 2 K), which is slightly suppressed with increasing temperature. The temperature dependence of magnetic susceptibility was measured as shown in Fig. 3(b). With decreasing temperature, the susceptibility experiences a sharp

FIG. 4. Photocurrent signals excited by light radiation with different wavelengths in $CaCu_3Fe_2Os_2O_{12}$ at room temperature. The inset shows the temperature dependence of resistivity.

FIG. 5. First-principles numerical results for the band structures and partial densities of states of $CaCu_3Fe_2Os_2O_{12}$.

behavior. The resistivity data cannot be fitted well with either the thermal active model or the Mott variable-range hopping mechanism. We therefore resorted to optical measurements to characterize the electrical feature. Figure 4 represents the values of photocurrent excited by optical radiation with various wavelengths at RT. When the optical wavelength decreases to about 1.35 μm, the signal of the photocurrent starts to sharply increase, revealing that the narrowest energy band gap in the polycrystalline CCFOO is roughly equal to 0.92 eV at RT. Note that in the present A- and B-site ordered CCFOO, the electrical transport is dominated by the corner-sharing Fe/OsO_6 octahedra. The observed Fe-Os antisite occupancy can thus possibly reduce the resistivity moderately.

The electronic structures of CCFOO were further investigated by the first-principles calculations. To determine the magnetic ground state, generalized-gradient approximation (GGA) and GGA $+ U$ spin-polarized calculations were performed for different magnetic structures. The GGA calculations always converge to the FiM $Cu^{2+}(\uparrow)Fe^{3+}(\uparrow)Os^{5+}(\downarrow)$ ground state regardless of the initial configuration. The GGA $+ U$ calculations using $U_{eff} = 5$ eV for Cu, 4 eV for Fe, and 2 eV for Os, following the common choices in the literature [9,11,14,39,40], also yield the same magnetic ground state, in agreement with experimental analysis. Other values of U_{eff} in a wide range around the above choices have also been tested and no qualitative change was found in the magnetic ground state. A total magnetic moment of 7.01 μ_B/f.u. is obtained by calculations, and the atomic contributions of Cu, Fe, and Os inside the muffin-tin spheres are 0.627, 4.043, and -1.421 μ_B, respectively. The values of the ionic magnetic moments are slightly reduced from their ideal values because of the strong hybridization with O-2p orbitals. Calculations with spin-orbit interactions yield only slight changes in the atomic spins to 0.603, 4.013, and -1.315 μ_B for Cu, Fe, and Os, respectively, with a total moment of 7.19 μ_B/f.u.

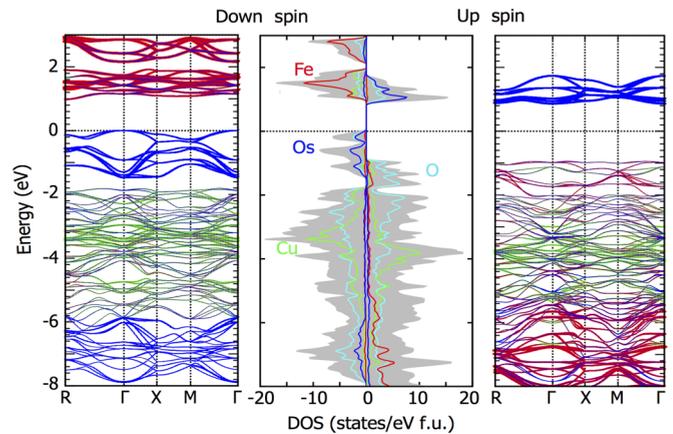Figure 5 shows the calculated electronic band structures and the partial densities of states with the above choices

of U_{eff}. The insulating nature of CCFOO is revealed: The majority spin has an energy gap of about 1.8 eV, whereas the minority spin has an energy gap of about 1.0 eV at the ground state, agreeing with the photocurrent measurement as shown in Fig. 4. The wide energy gap could provide protection to the high-temperature FiM ordering. Consistent with previous experimental analysis [9,41], in the present CCFOO, Cu^{2+} has one localized hole on its b_{1g} orbital, Fe^{3+} is fully polarized with a half-filled 3d-shell, and Os^{5+} has half-filled t_{2g} orbitals. The strong on-site Coulomb repulsion and Hund couplings should be responsible for the obtained energy gap. Note that the electronic states near the Fermi level are dominated by the Os-5d orbitals which hybridize strongly with the O-2p orbitals. It is therefore expected that appropriate element doping only on Os may tune the spin and electronic properties of the present high-T_C FiM insulator CCFOO. Actually, when the Os is replaced by Re, half-metallic behavior is observed in $CaCu_3Fe_2Re_2O_{12}$ [14].

To understand the high Curie temperature compared to that of Ca_2FeOsO_6, the magnetic exchange interactions of CCFOO were calculated using the spin model [42,43] $H = \sum_{(ij)} J_{ij} S_i \times S_j$, where S_i and S_j are the spin vectors of Cu, Fe, or Os ions at the sites i and j, respectively, and J_{ij} is the exchange interaction between the nearest-neighbor spin pair. Since previous calculations for Ca/Sr_2FeOsO_6 and $La/BiCu_3Fe_4O_{12}$ have shown that the exchange interactions J_{Fe-Fe}, J_{Os-Os}, and J_{Cu-Cu} between the neighboring atoms of the same type are relatively small and can be safely neglected [7,10,11,40,44], we consider here only three nearest-neighbor interactions, J_{Fe-Os}, J_{Cu-Fe}, and J_{Cu-Os} as shown in Fig. 6(b), and derive them by calculating the energy differences of the four magnetic configurations, i.e., FiM1, FiM2, FiM3, and FM1 mentioned before. These calculations yield $E(\text{FiM2} - \text{FiM1}) = 0.567$ eV/f.u., $E(\text{FiM3} - \text{FiM1}) = 0.692$ eV/f.u., and $E(\text{FM1} - \text{FiM1}) = 1.7$ eV/f.u. Obviously, the FiM1 spin structure with $Cu^{2+}(\uparrow)Fe^{3+}(\uparrow)Os^{5+}(\downarrow)$ coupling has the lowest energy. The derived AFM exchange interactions are $J_{Cu-Fe}S_{Cu}S_{Fe} = 9.19$ meV, $J_{Fe-Os}S_{Fe}S_{Os} = 32.8$ meV, and $J_{Cu-Os}S_{Cu}S_{Os} = 38.0$ meV, revealing a strong spin coupling between the A'-site Cu ions and the B'-site Os ions.

Previous studies for Ca_2FeOsO_6 [9,11] have yielded a similar exchange interaction between the B-site Fe and Os ions
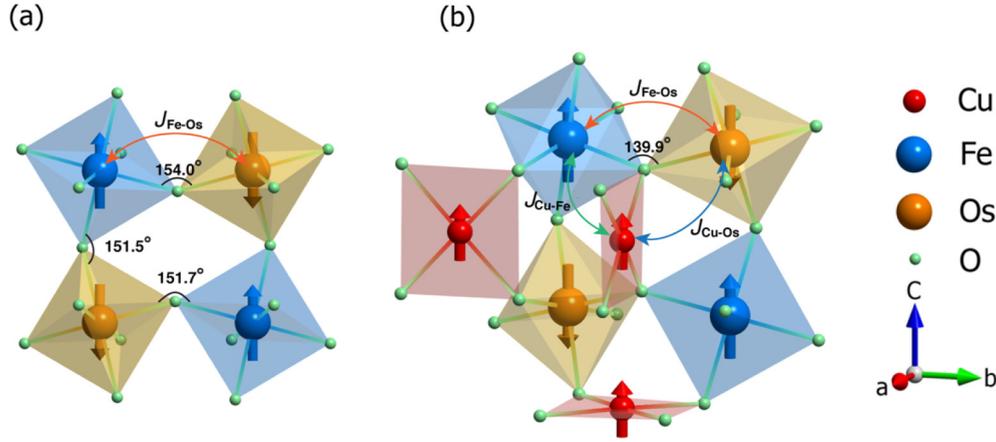
FIG. 6. (a) Magnetic interactions in the B-site-only ordered Ca_2FeOsO_6 between Fe and Os ions. (b) Magnetic interactions in both A-site and B-site ordered $CaCu_3Fe_2Os_2O_{12}$ among Cu, Fe, and Os ions.

with $J_{Fe-Os}S_{Fe}S_{Os} = 31$ meV [see Fig. 6(a)], indicating that the variations in bond length ($d_{Fe-Os} = 3.713$ Å for CCFOO and 3.855 Å for Ca_2FeOsO_6) and bond angle ($\angle$Fe-O-Os $= 139.9°$ for CCFOO and $152.4°$ for Ca_2FeOsO_6 in average) cannot be primarily responsible for the sharp enhancement of the Curie temperature from 320 K in Ca_2FeOsO_6 to 580 K in CCFOO. The enhancement thus should be associated with the introduction of the A'-site Cu^{2+} magnetic ions. As shown in Fig. 6(b), all the exchange interactions in CCFOO are mediated through the O ions and their values are proportional to the hybridization integral of the magnetic ions with the O $2p$ orbitals and inversely proportional to the Coulomb energy (plus the charge transfer energy). Because the Os $5d$ orbitals are more extended and locate near the Fermi energy and have a smaller on-site Coulomb interaction as well as a stronger hybridization with the O $2p$ orbitals, the spin couplings to the Os spins, i.e., the $J_{Fe-Os}S_{Fe}S_{Os}$ and $J_{Cu-Os}S_{Cu}S_{Os}$, are relatively stronger as derived in our numerical calculations. In contrast, the coupling between Cu and Fe ($J_{Cu-Fe}S_{Cu}S_{Fe}$) is much smaller considering that the Cu $3d$-hole orbital is more localized with a large Coulomb interaction and the half-filled Fe $3d$ orbitals are pushed further away to higher energies and hybridize less with the O $2p$ orbitals. Therefore, introducing the A'-site Cu^{2+} ions provides an additional Cu($\uparrow$)Os($\downarrow$) AFM coupling as strong as that of the B-site Fe($\uparrow$)Os($\downarrow$). Note that this also introduces slight magnetic frustrations because of the Cu($\uparrow$)Fe($\downarrow$) AFM interaction. However, it is the much stronger $Cu^{2+}(\uparrow)Os^{5+}(\downarrow)$ and $Fe^{3+}(\uparrow)Os^{5+}(\downarrow)$ AFM exchange energies that dominate the weaker $Cu^{2+}(\uparrow)Fe^{3+}(\downarrow)$ interaction and lead to the $Cu^{2+}(\uparrow)Fe^{3+}(\uparrow)Os^{5+}(\downarrow)$ long-range ferrimagnetic spin order. Thereby, the present A- and B-site ordered perovskite CCFOO has a much higher T_C (580 K) relative to that of the A-site nonmagnetic Ca_2FeOsO_6 ($T_C = 320$ K). In theory, the Curie temperature can be estimated within the mean-field approximation by solving the equation [42,43]

$$\langle S_i^z \rangle = \frac{S_i(S_i+1)}{3k_BT} \sum_j J_{ij}\langle S_j^z \rangle.$$

The T_C is given by the largest eigenvalue of the matrix $\Theta_{ij} = S_i(S_i+1)J_{ij}/3k_B$. Here k_B is the Boltzmann constant. We

obtain the $T_C = 1800$ K for CCFOO, which is also much higher than that estimated for Ca_2FeOsO_6 ($\sim$600 K) [11].

Here we point out that recent experimental studies reveal intriguing spintronic properties such as spin Seebeck, spin wave, spin transfer, and spin pumping in FM/FiM insulators as those observed in FM metals [45–49]. Moreover, since there is no moving charge in magnetic insulators, the dissipative losses associated with the magnetization dynamics are often exceptionally low. It means that a FM/FiM insulator with a high spin ordering temperature ($>$RT) and a wide energy band gap is favorable for possible applications in spintronics. Although a few spinel oxides and B-site ordered DPs possess relatively high FiM transition temperatures, the related band gaps are usually too small ($<$0.5 eV) [41,50–52]. Fortunately, the present CCFOO simultaneously possesses a high T_C ($\sim$580 K) and a considerable energy band gap ($\sim$1.0 eV), providing a promising candidate for multifunctional spintronic devices with potential applications well above RT.

IV. CONCLUSIONS

In summary, a ferrimagnet $CaCu_3Fe_2Os_2O_{12}$ with a high spin ordering temperature of 580 K was prepared under high-pressure and high-temperature conditions. This compound crystallizes to both A-site and B-site ordered quadruple perovskite structure with space group Pn-3. The charge states are confirmed to be $Cu^{2+}/Fe^{3+}/Os^{5+}$, which are in an orderly distribution at fixed atomic sites. The introduction of A'-site Cu^{2+} leads to strong $Cu^{2+}(\uparrow)Fe^{3+}(\uparrow)Os^{5+}(\downarrow)$ FiM coupling, which is responsible for the high spin ordering temperature. The fully filled Os-$t_{2g}^{3\uparrow}$ orbitals dominate the electronic properties near the Fermi level and open the band gap, providing an opportunity for manipulating the magnetic and electrical properties by doping the Os site alone. Although the B-site chemical doping in a perovskite has already been widely studied for many years to increase the spin or charge ordering temperatures, there is little study on A-site substitution with magnetic transition metals. The present work provides a rare example on sharply enhancing the T_C by introducing additional magnetic ions at the A site.

[1] P. A. Lee, N. Nagaosa, and X. G. Wen, Rev. Mod. Phys. **78**, 17 (2006).

[2] M. B. Salamon and M. Jaime, Rev. Mod. Phys. **73**, 583 (2001).

[3] T. Takenaka and K. Sakata, J. Appl. Phys. **55**, 1092 (1984).

[4] J. Wang, J. B. Neaton, H. Zheng, V. Nagarajan, B. Ogale, B. Liu, D. Viehland, V. Vaithyanathan, D. G. Schlom, U. V. Waghmare, N. A. Spaldin, K. M. Rabe, M. Wuttig, and R. Ramesh, Science **299**, 1719 (2003).

[5] T. Kimura, T. Goto, H. Shintani, K. Ishizaka, T. Arima, and Y. Tokura, Nature **426**, 55 (2003).

[6] K.-I. Kobayashi, T. Kimura, H. Sawada, K. Terakura, and Y. Tokura, Nature **395**, 677 (1998).

[7] A. K. Paul, M. Reehuis, V. Ksenofontov, B. Yan, A. Hoser, D. M. Többens, P. M. Abdala, P. Adler, M. Jansen, and C. Felser, Phys. Rev. Lett. **111**, 167205 (2013).

[8] R. Morrow, R. Mishra, O. D. Restrepo, M. R. Ball, W. Windl, S. Wurmehl, U. Stockert, B. Büchner, and P. M. Woodward, J. Am. Chem. Soc. **135**, 18824 (2013).

[9] H. L. Feng, M. Arai, Y. Matsushita, Y. Tsujimoto, Y. Guo, C. I. Sathish, X. Wang, Y.-H. Yuan, M. Tanaka, and K. Yamaura, J. Am. Chem. Soc. **136**, 3326 (2014).

[10] S. Kanungo, B. Yan, M. Jansen, and C. Felser, Phys. Rev. B **89**, 214414 (2014).

[11] H.-B. Wang, S.-S. Zhu, X.-D. Ou, and H. Wu, Phys. Rev. B **90**, 054406 (2014).

[12] R. Morrow, J. W. Freeland, and P. M. Woodward, Inorg. Chem. **53**, 7983 (2014).

[13] S.-H. Byeon, S.-S. Lee, J. B. Parise, and P. M. Woodward, Chem. Mater. **18**, 3873 (2006).

[14] W. T. Chen, M. Mizumaki, H. Seki, M. S. Senn, T. Saito, D. Kan, J. P. Attfield, and Y. Shimakawa, Nat. Commun. **5**, 3909 (2014).

[15] S.-H. Byeon, M. W. Lufaso, and J. B. Parise, Chem. Mater. **15**, 3798 (2003).

[16] S. A. Larregola, J.-S. Zhou, J. A. Alonso, V. Pomjakushin, and J. B. Goodenough, Inorg. Chem. **53**, 4281 (2014).

[17] H. Fujii, M. Toyoda, H. Momida, M. Mizumaki, S. Kimura, and T. Oguchi, Phys. Rev. B **90**, 014430 (2014).

[18] S.-H. Beyon, S.-S. Lee, J. B. Parise, P. M. Woodward, and N. H. Hur, Chem. Mater. **17**, 3552 (2005).

[19] M. S. Senn, W. T. Chen, T. Saito, S. García-Martín, J. P. Attfield, and Y. Shimakawa, Chem. Mater. **26**, 4832 (2014).

[20] Y. W. Long, N. Hayashi, T. Saito, M. Azuma, S. Muranaka, and Y. Shimakawa, Nature **458**, 60 (2009).

[21] Y. W. Long and Y. Shimakawa, New J. Phys. **12**, 063029 (2010).

[22] Y. W. Long, T. Saito, T. Tohyama, K. Oka, M. Azuma, and Y. Shimakawa, Inorg. Chem. **48**, 8489 (2009).

[23] I. Yamada, K. Takata, N. Hayashi, S. Shinohara, M. S. Mori, S. Muranaka, Y. Shimakawa, and M. Takano, Angew. Chem., Int. Ed. **47**, 7032 (2008).

[24] X. Wang, Y. S. Chai, L. Zhou, H. Cao, C. Cruz, J. Y. Yang, J. H. Dai, Y. Y. Yin, Z. Yuan, S. Zhang, R. Yu, M. Azuma, Y. Shimakawa, H. Zhang, S. Dong, Y. Sun, C. Q. Jin, and Y. W. Long, Phys. Rev. Lett. **115**, 087601 (2015).

[25] A. C. Larson and R. B. Von Dreele, General structure analysis system (GSAS), Report No. LAUR 86-748 (Los Alamos National Laboratory, Los Alamos, NM, 1994).

[26] P. Blaha, K. Schwarz, G. K. H. Madsen, D. Kvasnicka, and J. Luitz, *WIEN2K: An Augmented Plane Wave+Local Orbitals Program for Calculating Crystal Properties* (Karlheinz Schwarz, Technische Universitat Wien, Wien, Austria 2013).

[27] N. Hollmann, Z. Hu, A. Maignan, A. Günther, L.-Y. Jang, A. Tanaka, H.-J. Lin, C. T. Chen, P. Thalmeier, and L. H. Tjeng, Phys. Rev. B **87**, 155122 (2013).

[28] M.-J. Huang, G. Deng, Y. Y. Chin, Z. Hu, J.-G. Cheng, F. C. Chou, K. Conder, J.-S. Zhou, T.-W. Pi, J. B. Goodenough, H.-J. Lin, and C. T. Chen, Phys. Rev. B **88**, 014520 (2013).

[29] Z. Hu, S.-L. Drechsler, J. Malek, H. Rosner, R. Neudert, M. Knupfer, M. S. Golden, J. Fink, J. Karpinski, G. Kaindl, C. Hellwig, and Ch. Jung, Europhys. Lett. **59**, 135 (2002).

[30] Z. Hu, C. Mazumdar, G. Kaindl, F. M. F. de Groot, S. A. Warda, and D. Reinen, Chem. Phys. Lett. **297**, 321 (1998).

[31] T. Haupricht, R. Sutarto, M. W. Haverkort, H. Ott, A. Tanaka, H. H. Hsieh, H.-J. Lin, C. T. Chen, Z. Hu, and L. H. Tjeng, Phys. Rev. B **82**, 035120 (2010).

[32] A. K. Paul, M. Jansen, B. Yan, C. Felser, M. Reehuis, and P. M. Abdala, Inorg. Chem. **52**, 6713 (2013).

[33] Y. Shimakawa, Inorg. Chem. **47**, 8562 (2008).

[34] Y. W. Long, T. Saito, M. Mizumaki, A. Agui, and Y. Shimakawa, J. Am. Chem. Soc. **131**, 16244 (2009).

[35] I. Yamada, K. Tsuchida, K. Ohgushi, N. Hayashi, J. Kim, N. Tsuji, R. Takahashi, M. Matsushita, N. Nishiyama, T. Inoue, T. Irifune, K. Kato, M. Takata, and M. Takano, Angew. Chem., Int. Ed. **50**, 6579 (2011).

[36] Z. Zeng, M. Greenblatt, M. A. Subramanian, and M. Croft, Phys. Rev. Lett. **82**, 3164 (1999).

[37] J. A. Alonso, J. Sánchez-Benítez, A. De Andrés, M. J. Martínez-Lope, M. T. Casais, and J. L. Martínez, Appl. Phys. Lett. **83**, 2623 (2003).

[38] K. Takata, I. Yamada, M. Azuma, M. Takano, and Y. Shimakawa, Phys. Rev. B **76**, 024429 (2007).

[39] X.-F. Hao, Y.-H. Xu, F. Gao, D.-F. Zhou, and J. Meng, Phys. Rev. B **79**, 113101 (2009).

[40] C. Lee, E. Kan, and M.-H. Whangbo, arXiv:0904.4809.

[41] Y. Krockenberger, K. Mogare, M. Reehuis, M. Tovar, M. Jansen, G. Vaitheeswaran, V. Kanchana, F. Bultmark, A. Delin, F. Wilhelm, A. Rogalev, A. Winkler, and L. Alff, Phys. Rev. B **75**, 020404 (2007).

[42] P. W. Anderson, *Theory of Magnetic Exchange Interactions: Exchange in Insulators and Semiconductors*, edited by F. Seitz and D. Turnbull, Solid State Physics Vol. 14 (Academic, New York, 1963), pp. 99–214.

[43] E. Şaşıoğlu, L. M. Sandratskii, and P. Bruno, Phys. Rev. B **70**, 024427 (2004).

[44] H. Li, S. Lv, X. Liu, and J. Meng, J. Comput. Chem. **32**, 1235 (2011).

[45] K. Uchida, J. Xiao, H. Adachi, J. Ohe, S. Takahashi, J. Ieda, T. Ota, Y. Kajiwara, H. Umezawa, H. Kawai, G. E. W. Bauer, S. Maekawa, and E. Saitoh, Nat. Mater. **9**, 894 (2010).

[46] B. Heinrich, C. Burrowes, E. Montoya, B. Kardasz, E. Girt, Y.-Y. Song, Y. Sun, and M. Wu, Phys. Rev. Lett. **107**, 066604 (2011).

[47] X. Jia, K. Liu, K. Xia, and G. E. W. Bauer, Europhys. Lett. **96**, 17005 (2011).

[48] Steven S.-L. Zhang and S. Zhang, Phys. Rev. Lett. **109**, 096603 (2012).

[49] H. Skarsvåg, A. Kapelrud, and A. Brataas, Phys. Rev. B **90**, 094418 (2014).

[50] H. Kato, T. Okuda, Y. Okimoto, Y. Tomioka, Y. Takenoya, A. Ohkubo, M. Kawasaki, and Y. Tokura, Appl. Phys. Lett. **81**, 328 (2002).

[51] A. G. Flores, V. Raposo, L. Torres, and J. Iniguez, Phys. Rev. B **59**, 9447 (1999).

[52] Z. Szotek, W. M. Temmerman, D. Ködderitzsch, A. Svane, L. Petit, and H. Winter, Phys. Rev. B **74**, 174431 (2006).